# Raman studies of three-dimensional foam

N. Goutev and Zh. S. Nickolov*
*Department of Quantum Electronics, Faculty of Physics, Sofia University, 5, James Bourchier Bul., 1164 Sofia, Bulgaria*
(Received 22 January 1996)

The structure of the thin liquid films in a stable three-dimensional foam (shaving cream) has been studied by Raman scattering. Two phases existing in the foam films are identified—lamellar and isotropic. The lamellar phase is an ordered multilayer structure (gel) of stearic acid molecules in all-trans conformation. This is proved by the shape of the Raman spectra in the C-H stretching region and by the values of a characteristic parameter determined from them—the intensity ratio $R$. The spectra in the C-C stretching and C-H bending regions support this conclusion as they show absence of features characteristic of gauche conformations. An analysis of the Raman spectra in the C-H bending and C-H stretching regions suggests that stearic acid molecules in the foam lamellar phase have a hexagonal packing. On the basis of Raman spectroscopic data we propose a model of foam molecular structure and its evolution. According to it, small bilayer lamellae dispersed in the foam films after foam formation gradually self-organize around the bubbles in large shell-like bilayer structures. This arrangement is induced initially by the gas-liquid interfaces of the bubbles and consequently by the interfaces of the bilayer structures with the foam liquid. The process of organization of small lamellae into large bilayer structures can be followed by changes in the intensity ratio $R$ of the C-H band and in the half-width of the antisymmetric C-H stretching fundamental $d^-$. The investigations carried out in this work demonstrate the capabilities of Raman spectroscopy to study the microstructure of three-dimensional foams and their dynamics. Raman spectroscopic studies can be employed to study aging of foams on the molecular level and can be possibly extended to characterization of factors affecting foam stability. [S1063-651X(96)08307-9]

PACS number(s): 82.70.Rr, 78.30.−j, 68.15.+e

## I. INTRODUCTION

Dispersions of liquids in liquids (emulsions) and dispersions of gases in liquids (foams) occur widely in nature and have applications in a large range of technologies [1]. Foams in particular are of great scientific interest as exemplars of disordered cellular materials. Propagation of light in foams can be regarded as diffusive, i.e., due to multiple scattering [2]. Because of the strong parasitic scattering of light which masks the useful signal, Raman spectroscopic studies of three-dimensional foams have been highly obstructed and, as far as we know, have not been reported to date in the literature.

In foams the gas bubbles are separated by relatively thin liquid films (LF). As any other material system, foam preserves its structure only when it cannot easily be transformed into a system possessing lower energy. The molecules at the interfaces separating the bubbles from the thin films have a higher energy than the molecules in the bulk of the films due to surface pressure and that is why the surface of the bubbles is thermodynamically not stable. So over time foam evolves in such a way as to lead to a minimum total interface of the liquid films. Foam evolution is described by several processes. The most important are coarsening of foams due to diffusion of gas from the smaller bubbles to the larger bubbles, and drainage of the liquid in between the bubbles due to gravity along the so-called Plateau channels [3]. The first process is explained by the existence of pressure differences between bubbles of different sizes and leads to a decrease in the total surface area with time. It begins right after the formation of foam from solution and continues throughout its lifetime. The drainage of the liquid between the bubbles and subsequent coalescence of adjacent bubbles (or rupture of the bubbles when the liquid lamellae between them become too thin) are observed on a longer time scale (from several h to 1–3 days after formation for commercial foams, depending on foam type). When the liquid films are very thick the bubbles are spherical (wet foam), while after sufficient time for coarsening and partial drainage of the foam liquid, the films become thinner and the foam is composed of polyhedral bubbles. Eventually the foam becomes dry—the films are very thin, reaching tens of nanometers. The structure of the thin liquid films is the determining factor for the stability of foams [4]. In this respect Raman spectroscopic studies of three-dimensional foam would be of great interest because they can supply information about the molecular structure of the foam films.

If a laser beam impinges on three-dimensional foam in a cell it will undergo diffusive propagation and as a result a specific distribution of the excitation which we may term diffusive excitation is created in the volume. This excitation will create a volume distribution of the elementary Raman scattering centers with the same shape as that of the diffusive excitation. The Raman signal will undergo a secondary diffusion in all directions and as a result will reach the foam-cell boundaries. Thus Raman signals from the bulk foam could be detected. The specific dimension of the Raman intensity distribution at the surface of the foam, which is imaged on the spectrometer, is proportional to the transport mean free path of photons in foam $l^*$. The latter has been connected with the size $d$ of the bubbles—$l^* = 3.5d$ [2]. When $d$ increases the dimension of the Raman intensity source in foam broadens and its maximum decreases. As a

*Electronic address: znsof@phys.uni-sofia.bg

 

result the brightness of the image on the entrance slit of the spectrometer decreases and the detected Raman signal decreases too. Thus in order to have optimum Raman signal collection $l^*$ should match the most frequently used spectral slit widths. This means that the mean bubble size should be of the order of tens of micrometers. These are characteristic dimensions for some commercial foams and for fresh shaving foam in particular [5].

## II. EXPERIMENT

As in some recent investigations [2,5–7], we have chosen to study Gillette shaving foam [8] because it provides highly reproducible and stable samples. The stability of the foam is not of primary importance for a modern Raman experiment, but it should last for a period of time comparable to the time necessary to obtain an acceptable signal-to-noise ratio after signal averaging. According to [6] the period necessary for noticeable changes in Gillette foam rheology due to bubble growth is some 10 min after foam formation. Thus the time we need to obtain a Raman spectrum truly reflecting eventual changes in foam microstructure should be of the order of 1–3 min. This implies that only parallel spectral registration is feasible.

Gillette foam is produced after expansion at atmospheric pressure of a pressurized mixture of an aqueous solution of triethanolamine stearate with smaller amounts ($<1\%$) of sodium lauril sulphate (SLS) and polyethylene glycol-(23) lauril ether, together with emulsified liquid hydrocarbon gases [2]. The volume fraction of the bubbles in this foam is some $(92\pm1)\%$ [2].

Raman spectroscopy experiments were performed in backscattering, the laser beam making an angle of 50° with the cell. The foam was placed in a closed glass rectangular cell ($2\times2\times3$) cm to prevent changes due to evaporation, or was probed directly in the case of its dry or semidry residue. The liquid that drained off the foam was studied in 2 mm internal diameter capillaries in the conventional 90° geometry with the laser beam parallel to the long axis of the capillaries. The scattered signal was collected by an $F=40$ cm lens, passed through a Raman notch filter (Kaiser Optical Systems Inc.) and imaged on the entrance slit of a single 60 cm focal length polychromator. Detection of spectra was accomplished by an intensified vidicon (ISIT) and computer controlled multichannel system (OSA, B&M Spectronic). Excitation was with the 488 nm line of an argon ion laser (Zeiss-Jena) with typically 120 mW focused at the sample with an $f=100$ mm lens. The detection system was calibrated by Ne emission lines; the spectra are reproducible to $\pm0.5$ cm$^{-1}$. The spectra in the C-H stretching region were Fourier deconvoluted to enhance resolution using a procedure which has been described elsewhere [9].

Due to very high scattering of the foam the direct detection of Raman signal even in the region of the strong C-H stretching band (2800–3000) cm$^{-1}$ yielded a poor quality spectra at any stage of the foam evolution. In order to overcome these difficulties we employed a shifted detection difference method. This consists of taking the difference between two spectral recordings of the multichannel analyzer. In the first recording the Raman spectrum of a characteristic molecular vibration is present (for example, the C-H stretching band), although very weak, superimposed on the much stronger parasitic background reaching the detector. In the second a stepping motor effected an accurately controlled wavelength displacement so that the relevant Raman band was not imaged on the multichannel detector. As the parasitic scattered background is essentially the same, a difference between these two recordings results in a Raman spectrum of a good quality, which was further improved using Fourier smoothing. The shift for the C-H region was of the order of the free spectral coverage of the detection system — 400 cm$^{-1}$. A confirmation of the correctness of this experimental procedure is that the resulting spectra have essentially no background and at both ends approach the zero level.

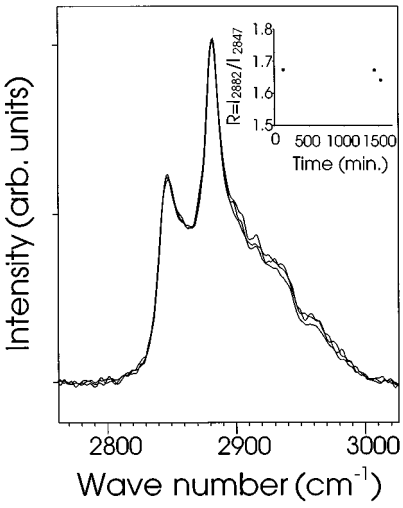


FIG. 1. Raman spectra of constant density foam in the C-H stretching region.The time dependence of the intensity ratio of the main peaks $R=I_{2882}/I_{2847}$ is shown in the inset.

## III. RESULTS

We have investigated Raman spectra of three-dimensional foam in the region of the C-H stretching vibrations, (2800–3000) cm$^{-1}$, in the region of the skeletal C-C stretching modes, (1050–1150) cm$^{-1}$, and in the (400–1500) cm$^{-1}$ methelene deformation region. In these regions the main contributions come from the vibrational modes of the long hydrocarbon ''tails'' (acyl chains) of the surfactant molecules in the foam. As surfactant molecules play a central role in the formation and stabilization of foam, an analysis of their spectra can provide information on chain packing, chain mobility, and chain conformation [10–14]. Thus a picture of molecular structure in foam can be constructed.

We have studied the changes in the Raman spectra of foam during aging for two separate cases. First, foam from the first 10–50 g expelled from a can, which is of constant density [15] and gives reproducible samples, was studied. This is, we believe, a very stable foam as drainage of liquid was very difficult to observe in the first 24 h. Examples of Raman spectra in the C-H region at different stages of aging such a sample of Gillette foam in a cell up to 24 h are shown in Fig. 1. Comparison between the spectra shows that the changes in the shape of the C-H band are insignificant, if noticeable at all. A simple quantitative criterion, which is

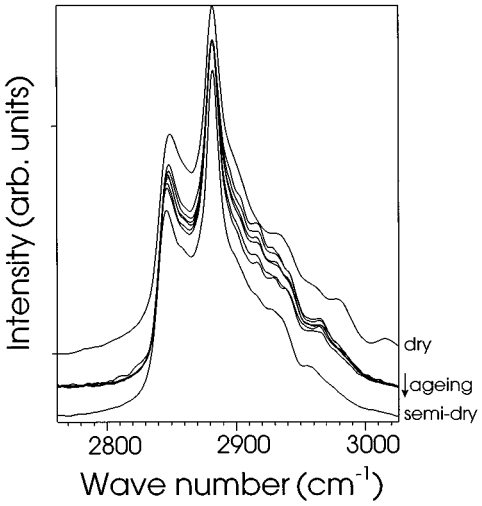


FIG. 2. Examples of Raman spectra in the C-H stretching region at different stages of ageing a sample of ''wet'' foam in a cell up to 72 h and of the dry and semidry foam residue. For more details see text.

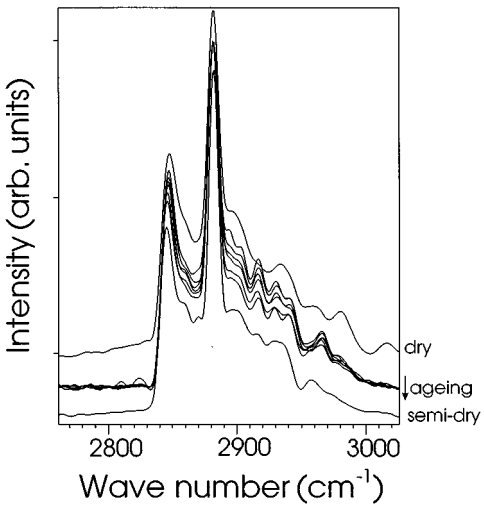


FIG. 3. Fourier deconvoluted analogs of spectra in Fig. 2.

generally used to measure lateral order of hydrocarbon chains and gives information on chain packing and chain mobility, is the ratio $R$ of the intensities of the components at 2882 and 2847 $cm^{-1}$. $R = I_{2882}/I_{2847}$ is plotted in the inset to Fig. 1 and clearly demonstrates the lack of spectral changes. Its average value is around 1.67. Generally this behavior suggests preservation of the structure of the thin liquid films on the molecular level. Consequently the Raman signal comes from a very stable foam in which the structure of the foam films does not change. Recent studies of wet foams with electronic spin resonance (ESR) obtained from a water solution of sodium dodecyl sulphate (SDS) [16] show significant changes in foam molecular structure with aging. This suggests that Gillette foam from the last 20% from the volume of the can, in which the liquid content should be higher, would be more influenced by aging and possibly provide Raman spectral evidence about changes in the structure of the liquid films.

We have studied the changes in the Raman spectra of ''wet'' foam from the bottom of the can during aging by taking consecutive recordings at 30 min intervals starting from formation of fresh foam to the first 6 h of aging, and then at 24 h intervals to a foam aged 72 h. For comparison purposes we have also investigated the Raman spectra of the liquid that drained off the foam. The Raman spectra of dry foam residue (the substance remaining after evaporation of all the liquid from the foam, approximately five days after leaving a fresh foam in the open at room temperature) have also been investigated. Raman spectra of semidry foam residue have also been studied—semidry meaning foam residue which still has some of the liquid in it after being left in the open. The aging of semidry foam residue at the time of the experiments was 24 h. Due to the diffusive excitation all Raman spectra of foam and dry residue reported in this work were completely depolarized, so we have not tried to analyze isotropic and anisotropic spectra.

Examples of Raman spectra in the C-H region at different stages of aging a sample of Gillette foam in a cell up to 72 h are shown in Fig. 2, together with the spectra of the dry and semidry foam residues. Figure 3 shows their Fourier deconvoluted analogs. A correlation between the changes in liquid film thickness with aging and our spectroscopic data could be very helpful but was not possible to establish as measuring film thickness in three-dimensional (3D) foam is a difficult task. Measuring liquid film thickness can usually be accurately performed only for model single liquid films [17].

Six superimposed bands can be distinguished in the C-H stretching region, Fig. 3. Their assignment according to a number of studies of polymethelene chains, $n$-paraffins, and surfactants in this spectral region [10–14] is as follows. The main peaks at 2847 $cm^{-1}$ and 2882 $cm^{-1}$ correspond to the symmetrical ($d^+$) and the antisymmetrical ($d^-$) $CH_2$ stretching modes, respectively. The components around 2935 and 2960 $cm^{-1}$ are assigned to the antisymmetrical and the symmetrical stretching vibrations of the terminal $CH_3$ groups. The band at 2935 $cm^{-1}$ also contains contributions due to Fermi resonance interaction between the symmetric methelene stretching mode $d^+$ and the continuum of overtones of the bending modes, $\delta(CH_2)$ [10]. The 2900 $cm^{-1}$ band, which is better observed in the deconvoluted spectra, is due to Fermi resonance interaction between the components mentioned above. The side component at 2916 $cm^{-1}$, which is resolved in the deconvoluted spectra, can be observed only in the C-H stretching spectra of foam aged in a cell. The same band, not so well expressed, is observed in the spectra of the semidry foam residue. It is not seen in the deconvoluted spectra of the dry residue.

The Raman skeletal C-C stretching region (1050–1150) $cm^{-1}$ is most convenient to analyze changes in the intramolecular conformations (trans vs gauche) within the acyl chains [18]. Two intense peaks at approximately 1063 and 1131 $cm^{-1}$ are due to the C-C vibration modes in the all-trans configuration, assigned to the in-phase C-C stretching and the out-of-phase C-C stretching, respectively. Another peak, less intense, observed in the case of phospholipid bilayers at around 1100 $cm^{-1}$ [19], is assigned to the crystalline C-C stretching mode. It possesses a strong chain-length dependence, with the wave number decreasing as the chain shortens [20]. As gauche conformers are induced, for example by changes in temperature or chain perturbations, a feature at 1085–1095 $cm^{-1}$ appears [19]. The ratio between

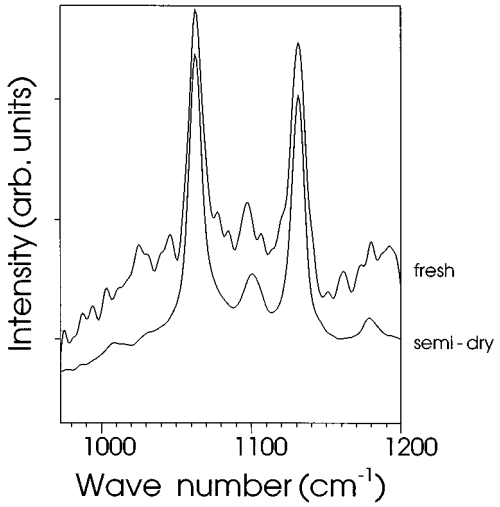


FIG. 4. Examples of Raman spectra of fresh foam in a cell and of the semidry foam residue in the C-C vibrations range. For more details see text.

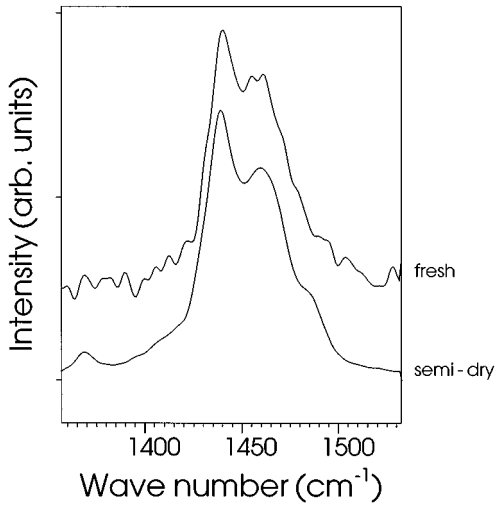


FIG. 5. Examples of the Raman spectra of fresh foam and of the semidry foam residue in the methelene C-H bending region. For more details see text.

the intensities at 1090 and 1131 $cm^{-1}$ ($I_{gauche}/I_{trans}$) can be used to monitor conformational changes in this region. Figure 4 shows examples of spectra recorded in the C-C vibration range of foam aged in a cell and of semidry foam residue. These spectra are also representative of the spectra of foam with constant density from the first 10–50 g expelled from a can. Our sensitivity in this vibrational region is very low due to the low scattering activities of the vibrations, and any changes in the spectra are less than the experimental scatter. It is clear that the two components at 1063 and 1131 $cm^{-1}$ dominate the spectra, while the $\sim$1090 $cm^{-1}$ component, indicating the presence of gauche conformers, is not observed. In the spectra of semidry foam residue the 1100 $cm^{-1}$ component is well observed, but is small in intensity. As a whole the observed Raman spectra in the C-C stretching region suggest that most of the acyl chains in foam are in the all-trans conformation.

Another informative vibrational region is (1400–1500) $cm^{-1}$. Here the comparatively strong methelene deformation features fall in the same wave number intervals as the weaker methyl symmetric and asymmetric bending modes, but the main contribution to the Raman spectra is due to the methelene vibrations. Moreover a manifold of two-phonon states (first overtone states) of the 720 $cm^{-1}$ rocking modes enter in Fermi resonance with the $CH_3$ bending modes. The methelene modes sensitively reflect changes in the lipid chain packing characteristics for the gel and liquid crystalline phases in both Raman and infrared spectra of membrane assemblies [21,22]. Thus the feature at 1460 $cm^{-1}$ decreases in intensity at the gel-to-liquid crystalline phase transition and broadens into the shoulder of the 1440 $cm^{-1}$ component [19]. For perfect gauche structures the peak at 1460 $cm^{-1}$ should not exist [12]. Its appearance is the evidence of intramolecular coupling of trans structures and its intensity is proportional to their concentration. The characteristic features of foam spectra in the (1400–1500) $cm^{-1}$ range, Fig. 5, conform with the conclusion of an all-trans conformation drawn from the analysis of the C-C spectra. A component at around 1416 $cm^{-1}$, associated with the formation of an orthorhombic subcell for the acyl chains of polyethylene [21], is not observed in the spectra of foam. This can be used as supportive evidence for the lack of orthorhombic structural packing. A shoulder at 1485 $cm^{-1}$ is clearly observed in the spectrum of the semidry foam residue but its assignment is open to interpretation.

After about 2 h of ageing a clear transparent liquid drains off from the Plateau channels in ''wet'' foam. We obtained its polarized Raman spectra in a standard 90° geometry. The parallel and perpendicular spectra in the C-H stretching region are shown in Fig. 6. The C-H band is strongly polarized, demonstrating the absence of parasitic scattering in the liquid due to microscopic liquid crystals. A comparison of the intensities of the water Raman O-H stretching band and the C-H band in foam and in the liquid showed that water is the dominant constituent in the drained off liquid. The shape of the C-H band in the liquid (Fig. 6) is characteristic of dilute aqueous solutions of surfactants [23].

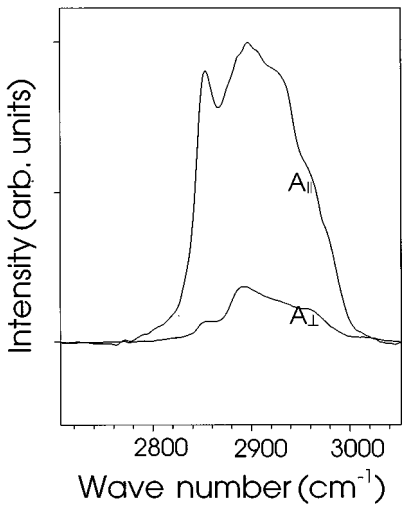


FIG. 6. Parallel $A_{\parallel}$ and perpendicular $A_{\perp}$ Raman spectra of the drained off liquid from Gillette foam in the C-H stretching region.

## IV. DISCUSSION

It is seen from the Raman spectra of ''wet'' foam in the C-H region (Figs. 2 and 3) that the band shape changes weakly with aging. Its subcomponents are comparatively well expressed in all stages of foam evolution and only their relative intensities change. This makes us suppose that we have a well defined molecular structure in Gillette shaving foam under these conditions, which does not significantly alter with aging. A more precise analysis of the structure of the C-H band can be done with the help of a quantitative parametrization describing it. The most widely used parameter is the ratio $R$ between the peak intensities of the fundamental modes $d^+$ and $d^-$ which, as already mentioned, gives information on conformational order and lateral packing of the acyl chains [10–14,24]. However, we should bear in mind the different behavior of both major modes in the C-H band of long chain amphiphiles. The $d^+$ fundamental is sensitive to the lateral packing of the acyl chains because of its Fermi resonance interaction with the continuum of $CH_2$ bending overtones, the latter being subject to significant intermolecular coupling. Its shape is associated with the specific type of crystallographic structure the chains can assume [10]. For the hexagonal structures it is characterized with a single narrow line at 2847 $cm^{-1}$, in contrast to the triclinic forms, which have two maxima (2855 and 2847 $cm^{-1}$), and to the orthorhombic-related structures having a slightly broader line at 2847 $cm^{-1}$ [10]. Unlike the $d^+$ mode which is sensitive to lateral order, the antisymmetrical methelene stretching mode $d^-$ is forbidden by symmetry to participate in Fermi resonance interactions so it is merely superimposed on the continuum of bending overtones $\delta(CH_2)$ without experiencing any change when they undergo intermolecular coupling and is insensitive to lateral packing. Most frequently $d^-$ is considered to reflect conformational disorder of the acyl chains although other information can also be extracted [14,25]. Having in mind the different behavior of the two major modes in the C-H band of long chain surfactants we should be very careful when we consider the ratio of the peak heights $R$ as a characteristic of both environment and conformational disorder of extended chains in foam. Nevertheless, values of 0.7 for completely melted chains in the liquid state, 1.5 for vibrationally decoupled all-trans chains, and 2.2 for highly ordered crystalline lattices have been accepted [26] and used successfully in a number of studies to determine structural changes in different complex systems. Using $R$ for characterization of Gillette foam we should also take into account the equimolar ratio of stearic acid and triethanolamine present. As the acid has 16 C-H oscillators and that of the amine has six, part of the Raman signal in the C-H region will be due to the amine. We tried to evaluate the influence of triethanolamine on the C-H Raman spectra of foam by comparing their spectra, Fig. 7. Apparently the presence of amine can increase the ratio $R$, because one of the peaks in its C-H parallel spectrum is at 2886 $cm^{-1}$. However, we assume that this change would not be significant as we do not observe the other two major components of the amine spectrum (2835 and 2950 $cm^{-1}$) in the spectra of foam (Fig. 7) and we can still correctly use $R$ for foam structure characterization.

In Fig. 8 is shown the dependence of $R$ on the time

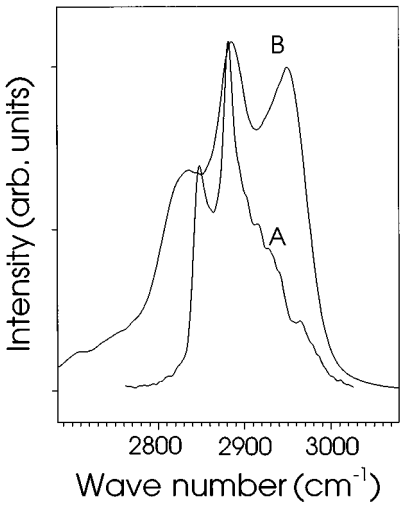


FIG. 7. Raman spectrum of ''wet'' foam aged in a cell (A) and parallel Raman spectrum of triethanolamine (B) in the C-H stretching region. The spectra are normalized to their intensity maxima.

elapsed from the formation of ''wet'' Gillette foam. The average value of $R$ is around 1.65. Values of $R$ close to these are characteristic of vibrationally decoupled hydrocarbon chains in the all-trans conformation. These have been observed in highly ordered polymethelene chains [10], as well as in multilayer Langmuir-Blodgett films ($R=1.47$ [27] and $R=1.44$ [28]), and in lamellar phases of surfactants in water solution [24]. Thus we can conclude that stearic acid molecules in foam are in the all-trans conformation and are organized in an ordered multilayer or crystal-like structure. This is confirmed also by the appearance of the spectra of foam and dry foam in the C-C stretching and C-H bending regions (Fig. 4 and Fig. 5) and agrees with the fact that the hydrocarbon tails of stearic acid molecules melt at 68 °C, well above the temperature (24 °C) at which we have performed the experiments.

Having assumed that an ordered phase exists in foam we can try to determine the type of lateral molecular packing. The shape of the $d^+$ mode, a single band (Fig. 2, Fig. 3), shows that we have either hexagonal or orthorhombic packing. The spectra in the bending region show that an orthorhombic lattice is not present as the line at around 1420 $cm^{-1}$, which is characteristic of this type of packing

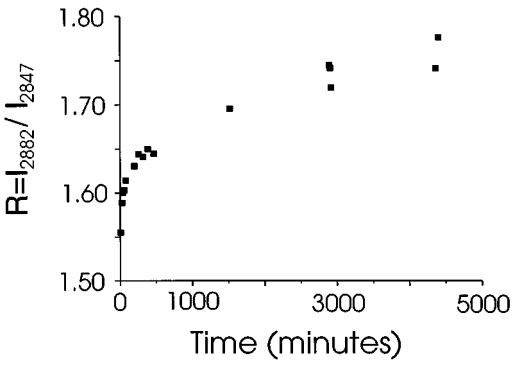


FIG. 8. Dependence of the intensity ratio $R$ of the C-H stretching band on the time elapsed from formation of ''wet'' foam.

[12,21,24], is not detected, Fig. 5. Therefore hexagonal packing of stearic acid molecules in all-trans conformation apparently exists in Gillette foam. This conclusion can be further substantiated by the appearance of the component at 2916 $cm^{-1}$ in the C-H spectra of foam. Its wave number is close to the assignment of the $d^-(\pi)$ fundamental in the IR C-H stretching spectra of extended polymethelene chains (2920 $cm^{-1}$, [10]) and it coincides with the observed $d^-(\pi)$ mode in the IR spectrum of the gel state of octadecyltrimethylammonium chloride in water at 24 °C [25]. It is natural to suppose that it is observed in the Raman spectrum because of breaking of selection rules [29]. A similar effect is connected with such changes in the symmetry of the molecule or in the crystal field in which it interacts, when the new symmetry group does not include a center of symmetry. The component at 2916 $cm^{-1}$ has been observed in the Raman spectra of some of the organized amphiphilic systems mentioned above [24,28], and its appearance is connected with the presence of gauche conformations which change the symmetry of the molecule. As we have shown that stearic acid molecules in foam are in the all-trans conformation they have a group of symmetry $C_{2h}$, including a center of inversion [28]. Therefore if selection rules are weakened the site group of the molecule should not have such a center. This is so for hexagonal packing but not for orthorhombic [29].

The studies of Friberg and Langlois [30] show that in a solution having the same composition as the foam forming solution (stearic acid:triethanolamine in a molar ratio 1:1), with the exception of the additives, two phases can exist—lamellar and isotropic. Combined with our spectroscopic observations this gives us enough ground to assume that the highly organized ordered crystal-like structure in foam is due to formation of a lamellar phase in the thin liquid films. The Raman spectroscopic evidence suggests that the molecules of the stearic acid are organized in this phase situated in the sites of a hexagonal crystal lattice and are in the all-trans conformation. Similar lamellar phases are referred to as gels [19].

It is interesting to consider the role of the amine in the organization of the lamellar phase. Some suggestions can be drawn by the analysis of the half-widths of the $d^-$ fundamental in the Raman spectra of the C-H band. The size of the unit cell in the crystal lattice of surfactants in the solid state determines the ability of the hydrocarbon chains to rotate and twist [10,14,25]. According to these studies of the C-H band it is suggested that the motion of the chains is connected with the half-width of the $d^-$ mode [14,25] — the higher the freedom of rotation around the axis of the chains the greater the width. In Fig. 9 is shown the dependence of the half-width of the $d^-$ mode on the aging of ''wet'' foam. The mean value is about 12 $cm^{-1}$. It is greater than the characteristic half-width of 9 $cm^{-1}$ for long hydrocarbon chains in a hexagonal packing [10]. It is also greater than the half-widths of the $d^-$ mode (11 $cm^{-1}$) in Langmuir-Blodgett multilayers of Cd and Ba stearates [27,28]. In Langmuir-Blodgett multilayers [27,28] the freedom of rotation of the surfactant molecules is limited, because of the small size of the surfactant head groups, which bring the tails closer to each other. In foam the greater half-widths suggest that the motion of the acyl chains is not restricted to such an extent and is probably due to a bigger size of the ''heads'' of the

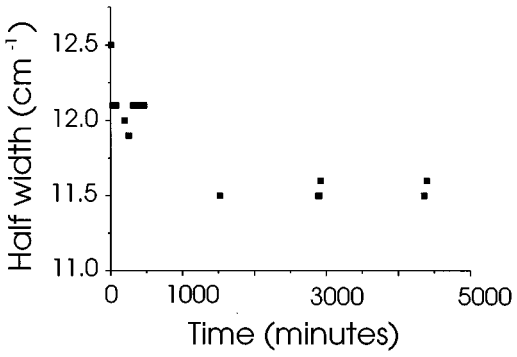


FIG. 9. Time dependence of the half-widths of the asymmetrical C-H stretching fundamental $d^-$.

amphiphilic compounds. One possible explanation of the increase in the size of the ''heads'' is that the majority of triethanolamine molecules are connected as a second layer to stearic acid molecules of the bilayers. Thus a possible model of the molecular structure of the foam gel could be based on the following assumptions. When the triethanolamine stearate is dissolved in water it will dissociate to acid and amine. At the composition of the foam forming solution and at room temperature, stearic acid molecules, driven by hydrophobic interaction, will arrange in bilayers with their hydrocarbon chains inside. The ionic head groups of the acid and amine will attract each other. A layer of triethanolamine with its O-H groups oriented outwards will be formed over the bilayer. The separate triethanolamine molecules are connected to each other in this layer by hydrogen bonds with water molecules serving as bridges between them. Thus each of these complex bilayers has a hydrophilic surface and is not charged. In view of the spectroscopic evidence we can also assume that there is a long-range ordering in the lamellar phase which is facilitated by the presence of water in the system. Water molecules in the bulk are connected with a network of hydrogen bonds. It is not disrupted in gel phases [27,31] and serves as the connecting media between acid-amine bilayers. This is supported by the changes in the C-H stretching Raman spectra in the transition from foam to semidry and dry foam residue, Fig. 2 and Fig. 3. It is evident that as the water content in foam decreases and finally becomes zero the component at 2916 $cm^{-1}$ and the substructure of the bands around 2900, 2935, and 2960 $cm^{-1}$ disappears. This can be explained by the disruption of hydrogen bonds which support the ordering in the amine layers and in the system as a whole.

The analysis of the Raman data so far shows that Gillette foam can be considered as comprising two phases—isotropic liquid and a liquid crystalline phase (gel). Our Raman studies of aging show that foam has the ability to retain the liquid crystalline phase without significant changes in the structure of the thin LF while the isotropic liquid is gradually released along Plateau's channels. This makes us believe that the anisotropic phase is strongly connected to the surface of the bubbles. The following simple experiment supports this assumption. We filled two 2 mm diam capillaries with fresh foam and sealed them hermetically. In about 2 h columns of clear transparent liquid about 5 mm high drained to the bottom of the capillaries. At that moment a swift turn to 180° of

one of the capillaries caused bubbles from the foam to move upwards through the liquid. After this the liquid appeared very cloudy. When the same experiment was repeated with the other capillary after a 24 hour period cloudiness of the drained off liquid was not observed. These observations can be explained if we assume that in fresh liquid films there is a dispersion of discoidal bilayer lamellae. When the capillary is turned upside down bubbles with loosely attached lamellae float upwards, then the lamellae are gradually released and mix with the liquid, inducing turbidity. After 24 h, the lamellae organize in multilayer structures similar to liposomes, strongly connected to the surface of the bubbles, so turbidity is not observed.

It is well known that interfaces of the gas-liquid type have a noticeable orientational effect on lamellar phases [31]. The connection of the bilayer lamellae to the surface of the bubbles after a characteristic period of time could be explained by the gradual orientation of the small lamellae parallel to the interface and their subsequent organization in large bilayer structures. This effect should be the driving force of the evolution of molecular structure of foam as foams are characterized with an enormous surface area (gas-liquid) per unit volume. Let us make an approximate evaluation of $S$—the surface area in 1 $cm^3$ of Gillette foam. In 1 $cm^3$ of fresh foam there is a volume fraction $V_g$ of gas (spherical bubbles with diameter $D_b$) and a volume fraction $V_l$ of liquid. The gas is contained in $N=6V_g/\pi D_b^3$ bubbles, which are separated from the thin liquid films by an interfacial area of $S=N\pi D_b^2=6V_g/D_b$. The bubbles in fresh Gillette foam have a mean diameter of about 20 $\mu$m and as the gas fraction is $V_g=0.92$ $cm^3$ [2] then in 1 $cm^3$ of Gillette foam we will have about $200\times10^6$ bubbles with $S=3000$ $cm^2$. For comparison a cubic ''drop'' of liquid with the same volume (80 $\mu$l) as the liquid in 1 $cm^3$ of Gillette foam, but not organized in foam, will have surface area of only 1.1 $cm^3$.

The ordering of the lamellar phase around the surface of the bubbles can be explained by the following simple model. Right after foam formation the thin LF contain a dispersion of discoidal lamellar bilayers (lamellae) with finite sizes in an isotropic phase. Assume that the surface of every bubble pointing to the liquid films is hydrophilic, which is true for the possible configuration suggested above—stearic acid molecules connected with a layer of triethanolamine supported by hydrogen bonding with neighboring water molecules. To a first approximation we can assume that the bilayer lamellae do not interact with each other. There will be an interaction between the molecules at the gas-liquid interface and the lamellae in the LF which have the same hydrophilic surfaces. It can be described by the potential energy $U(z)$ which a single lamella with unit area attains in proximity to the interface. The potential energy $U^l$ of a single square bilayer with an area $S=d^2$ close to a hydrophilic interface, Fig. 10, is given by

$$U^l=\int_S U(z)dS. \tag{1}$$

Let us extend this expression in Taylor series around point $z_0$ (the middle of the lamella):

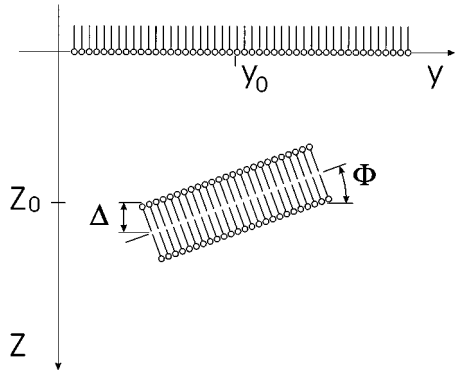


FIG. 10. A single bilayer lamella in proximity to the bubble surface.

$$U(z)=U(z_0)+U'(z_0)(z-z_0)+\frac{1}{2}U''(z_0)(z-z_0)^2+\ldots. \tag{2}$$

For small angles of rotation we have

$$(z-z_0)=(y-y_0)\Phi. \tag{3}$$

(1) Combining (1)–(3) we get

$$U^l=S\left(U(z_0)+\frac{1}{6}U''(z_0)\Delta^2\right), \tag{4}$$

where $\Delta=(d/2)\Phi$ is the displacement of the end of the lamella. We can assume that every lamella is a thermodynamical system in equlibrium with the isotropic phase at temperature $T$. The probability to find a lamella at a distance $z_0$ from the interface and rotated to an angle $\Phi$ in respect to the normal to the surface is given by Boltzmann's law:

$$P(z_0,\Phi)/P(\infty,0)=\exp\left\{-\frac{S}{kT}\left(U(z_0)+\frac{1}{6}U''(z_0)\Delta^2\right)\right\}. \tag{5}$$

It is clear that the lamellae are concentrated around the point $(z_{\min},0)$ for which we have $U(z_{\min},0)=U_{\min}$. The sharp maximum of this distribution depends essentially on the ratio $S/kT$. Thus bigger lamellae are better localized. For $S\to\infty$ (very big lamellae) we have ordering in a single layer with a definite position $z_{\min}$. In this way we have shown that an interface in foam induces ordering of bilayer lamellae into a large bilayer structure in its closest vicinity. This bilayer will similarly influence the remaining lamellae in the LF. Gradually multilayer shells of lamellae will be formed around the bubbles. The separate layers will be better localized if they consist of bigger lamellae. For our foam system the potential energy $U(z)$ can be described as a sum of two contributions:

$$U(z)=U_{\rm atr}+U_{\rm rep}, \tag{6}$$

where $U_{\rm atr}$ is the potential describing the van der Waals attraction forces acting between hydrocarbon phases at very large distances. For $U_{\rm atr}$ we have the well known formula [32]:

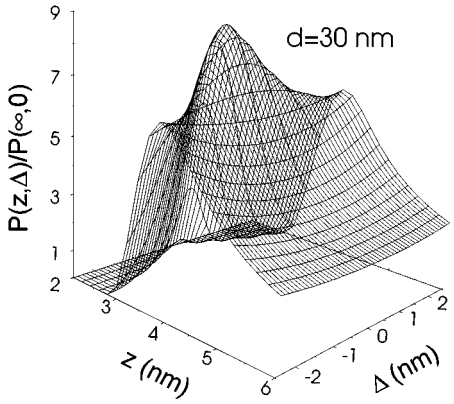


FIG. 11. Normalized probability density to find a lamella at a defined position in a foam liquid film (Fig. 10). Lamella size is $d=30$ nm.

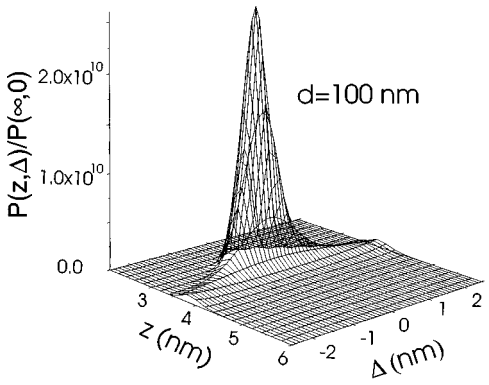


FIG. 12. Normalized probability density to find a lamella at a defined position in a foam liquid film (Fig. 10). Lamella size is $d=100$ nm.

$$U_{\mathrm{atr}}=-\frac{A}{12z^2}, \tag{7}$$

where $A$ is the Hamaker constant. For membranes of hydrocarbon tails it is of the order of $(4-7)\times10^{-21}$ J.

The repulsive forces between the separate lamellar bilayers in Gillette foam, which are supposed to act at close distances, can be hydration or steric in origin. Their character and their dependence on the distance between the bilayers have not been studied for the present system. Therefore we will assume a semiempirical description introducing the ratio

$$U_{\mathrm{rep}}/U_{\mathrm{atr}}=-\frac{2}{2+\alpha}\left(\frac{z_{\min}}{z}\right)^{\alpha}, \tag{8}$$

where $\alpha$ is a constant, which can be defined experimentally and depends on the type of repulsive forces. When $\alpha>0$ the repulsive forces will dominate at small distances. This expression for $U_{\mathrm{rep}}$ is realistic for some steric forces [31]. The coefficient $[-2/(2+\alpha)]$ was chosen for convenience in the analytical transformations. Combining (7) and (8) we have

$$U(z)=\frac{A}{12z^2}\left[\frac{2}{2+\alpha}\left(\frac{z_{\min}}{z}\right)^{\alpha}-1\right]. \tag{9}$$

It is seen from (9) that $z_{\min}$ is the distance at which the potential energy is minimum. An estimate of $z_{\min}$ can be obtained from [30], where it has been established that at maximum water content in the stearic acid–triethanolamine–water system the distance between the bilayers in the lamellar phase is 3 nm. Let us also assume the following values of the other parameters in (9): $A=5\times10^{-21}$ J, $T=24\,^{\circ}$C, $\alpha=4$.

We have calculated the probability density distributions $P(z_0,\Phi)/P(\infty,0)$ corresponding to the interaction potential $U(z)$ defined in (9), for two sizes of the discoidal lamellae—$d=30$ nm and $d=100$ nm. The results are shown in Fig. 11 and Fig. 12. It is evident that small lamellae are poorly localized and have a great freedom of rotation. When the size of the lamellae increases they are more strongly connected to the neighboring large surface (bubble or extended bilayer) and they have less rotational freedom, Fig. 12.

The process of discoidal lamellae growth can be followed by changes in $R$ and in the half-width of $d^-$. We have already established that the conformation of stearic acid is almost unchanged in the process of aging. This means that the changes in $R$ are due to changes in chain packing and chain intermolecular interactions. The increase of $R$ from 1.55 for fresh foam to 1.77 for foam aged 72 h suggests that the molecular organization of surfactant molecules evolves from an initial state of dispersed discoidal bilayers to big lamellar bilayers arranged around the surface of the bubbles. When we have a dispersion of small lamellae, part of the Raman signal is due to the molecules at their curved ends. These molecules do not take part in long-range interactions characteristic of the main crystal-like part of the lamellae. As a result their C-H stretching band will have smaller ratio $R$ than that of the C-H band, characterizing the vibrationally coupled molecules from the main body. When the lamellae group together the number of the molecules at their curved ends will decrease and $R$ will increase. A similar effect has been observed in dispersions of biological membranes [33]. The vibrationally decoupled end molecules have a greater motional freedom and their rotation and twisting should be more intensive. This is confirmed by the changes in the half-width of the $d^-$ mode with aging, Fig. 9. In fresh foam, where we assume a dispersion of lamellae, it is 12.6 $\mathrm{cm}^{-1}$ while at the end of the study, when we have large lamellar structures, it is 11.5 $\mathrm{cm}^{-1}$.

## V. CONCLUSION

The understanding of the properties of three-dimensional liquid foams in relation to their molecular structure is a challenging problem in the physics of dispersed systems. New experimental techniques applied in this field are needed for its solution. We have studied the structure of the thin liquid films and its evolution in a stable three-dimensional foam by Raman scattering and show that this is a method of great potential due to its noncontact nature and the ability to extract information about characteristic molecular vibrations.

Our results show that the two phases existing in foam films— lamellar and isotropic—can be easily identified by

their Raman spectra. An analysis of the Raman spectra in three different vibrational regions showed that the lamellar phase is in the gel state and is composed of amphiphilic molecules in the all-trans conformation with hexagonal lateral packing. A model of foam molecular structure and its evolution is proposed. Small bilayer lamellae, dispersed initially in the foam liquid, gradually self-organize in large closed multilayer structures around the bubbles. The arrangement is initially induced by the gas-liquid interfaces and after that by the interfaces of the larger bilayer structures with the foam liquid. This process of organization in shell-like structures can be followed by changes in the characteristic parameters of the C-H stretching Raman band. We suppose that the lamellar shells slow down gas diffusion between the bubbles and contribute to the stability of the foam.

Unstable foams and thin liquid films can also be investigated by Raman spectroscopy, but enhanced time resolution capabilities, high sensitivity, and high signal-to-noise ratio are necessary. Investigations of changes in the structure of the O-H Raman band would provide valuable insight into the dynamics of water in the confined geometry of the foam films and are of current interest in the the physics of complex fluids [34].

## ACKNOWLEDGMENTS

The authors gratefully acknowledge financial support by the Bulgarian National Science Foundation under Project No. F462. Z.N. thanks Professor J.C. Earnshaw for stimulating discussions and for critical reading of the manuscript.

[1] B. Vincent, in *Surfactants*, edited by Th.F. Tadros (Academic Press, London, 1984).
[2] D.J. Durian, D.A. Weitz, and D.J. Pine, Science **252**, 686 (1991).
[3] J.H. Aubert, A.M. Kraynik, and P.B. Rand, Sci. Am. **254**, 74 (1986).
[4] *Foams: Physics, Chemistry and Structure*, edited by A.J. Wilson (Springer-Verlag, London, 1989).
[5] D.J. Durian, D.A. Weitz, and D.J. Pine, J. Phys. Condens. Matter **2**, SA433 (1990).
[6] D.J. Durian, D.A. Weitz, and D.J. Pine, Phys. Rev. A **44**, R7902 (1991).
[7] J.C. Earnshaw and A.H. Jaafar, Phys. Rev. E **49**, 5408 (1994).
[8] The Gillette Company, 454 Basingstoke Road, Reading, Berkshire RG2 0QE, U.K.
[9] T. Kalkandjiev, V. Petrov, and J. Nikolov, Appl. Spectrosc. **43**, 44 (1989).
[10] R.G. Snyder, S.L. Hsu, and S. Krimm, Spectrochim. Acta Pt. A **34**, 395 (1978).
[11] R.G. Snyder and J.R. Scherer, J. Chem. Phys. **71**, 3221 (1979).
[12] S. Abbate, G. Zerbi, and S.L. Wunder, J. Phys. Chem. **86**, 3140 (1982).
[13] G. Zerbi and S. Abatte, Chem. Phys. Lett. **80**, 455 (1981).
[14] R.G. Snyder, H.L. Strauss, and C.A. Elliger, J. Phys. Chem. **86**, 5145 (1982).
[15] D.J. Durian, D.A. Weitz, and D.J. Pine, in *Complex Fluids*, edited by E.B. Sirota, D. Weitz, T. Witter, and J. Israelachvili, MRS Symp. Proc. No. 248 (Materials Research Society, Pittsburgh, 1992), p. 295.
[16] J.-M. di Meglio and P. Baglioni, J. Phys. Condens. Matter **6**, A375 (1994).
[17] *Thin Liquid Films, Fundamentals and Applications*, edited by I.B. Ivanov, Surfactant Science Series Vol. 29 (Dekker, New York, 1988), Chap. 11.
[18] J.L. Lippert and W.L. Peticolas, Proc. Natl. Acad. Sci. USA **68**, 1572 (1971).
[19] *Advances in Infrared and Raman Spectroscopy*, edited by R.J.H. Clark and R.E. Hetser (John Wiley & Sons, London, 1984), Vol. 11, Chap. 1.
[20] J.L. Lippert and W.L. Peticolas, Biochim. Biophys. Acta **282**, 8 (1972).
[21] N. Yellin and I.W. Levin, Biochim. Biophys. Acta **489**, 177 (1977).
[22] D.G. Cameron, H.L. Casal, E.F. Gudgin, and H.H. Mantsch, Biochim. Biophys. Acta **596**, 463 (1980).
[23] K. Kalyanasundaram and J.K. Thomas, J. Phys. Chem. **80**, 1462 (1976).
[24] M. Picquart, J. Phys. Chem. **90**, 243 (1986).
[25] T. Kawai, J. Umemura, T. Takenaka, M. Kodama, and S. Seki, J. Colloid Interface Sci. **103**, 56 (1985).
[26] B.P. Gaber and W.L. Peticolas, Biochim. Biophys. Acta **465**, 260 (1977).
[27] S.B. Dierker, C.A. Murray, and J.D. Legrange, Chem. Phys. Lett. **137**, 453 (1987).
[28] M. Harrand and M. Masson, J. Chem. Phys. **87**, 5176 (1987).
[29] W.A. Wooster, *Tensors and Group Theory for the Physical Properties of Crystals* (Clarendon Press, Oxford, 1973).
[30] S.E. Friberg and B.C. Langlois, Langmuir **10**, 2939 (1994).
[31] G.J.T. Tiddy, Phys. Rep. **57C**, 1 (1980).
[32] J. N. Israelachvili, in *Intermolecular and Surface Forces* (Academic Press, London, 1992), Chap. 16.
[33] M. Lafleur, J.L. Dasseux, M. Pigeon, J.Dufourcq, and M. Pezolet, Biochemistry **26**, 1173 (1987).
[34] Zh.S. Nickolov, J.C. Earnshaw, F. Mallamace, N. Micali, and C. Vasi, Phys. Rev. E **52**, 5241 (1995).